

A comparison of forest fire indices for predicting fire risk in contrasting climates in China

Xiaowei Li · Gang Zhao · Xiubo Yu · Qiang Yu

Received: 15 May 2013 / Accepted: 22 September 2013 / Published online: 5 October 2013
© Springer Science+Business Media Dordrecht 2013

Abstract The relationships between fire danger indices and fire risk have been extensively studied in many regions of the world. This work uses partial effect analysis in semiparametric logistic regression models to assess the nonlinear relationships among location, day, altitude, fire danger indices, normalized difference vegetation index (NDVI), and fire ignition from 1996 to 2008 in four different climatic regions in China. The four regions are North China (NR), Northeast China (NE), Southeast China (SE), and Southwest China (SW). The three main results are as follows: First, different fire danger indices are selected as significant variables dependent on the region. The inter-regional difference could be partially explained by difference in local weather and vegetation conditions. Second, spatial location exerts highly significant effects in all four regions. NDVI values are selected as explained variable for NR, NE, and SE on fire ignitions. On a daily scale, altitude influences fire ignition for NR, SE, and SW. Third, the robustness of the probability models used in NE, SE, and SW is better than that in NR on a daily scale. The semiparametric logistic regression model used in this study is useful for assessing the ability of fire danger indices to estimate probabilities of fire ignition on a daily scale. This study encourages further research on assessing the predictive ability of fire danger indices developed at other temporal and spatial scales in China.

X. Li · G. Zhao · Q. Yu

Key Laboratory of Water Cycle and Related Land Surface Processes, Institute of Geographic Sciences and Natural Resources Research, Chinese Academy of Sciences, Beijing 100101, China

X. Li · G. Zhao

University of Chinese Academy of Sciences, Beijing 100049, China

X. Yu

Key Laboratory of Ecosystem Network Observation and Modeling, Institute of Geographic Sciences and Natural Resources Research, Chinese Academy of Sciences, Beijing 100101, China

Q. Yu (✉)

Plant Functional Biology and Climate Change Cluster, School of the Environment,
University of Technology, Sydney, PO Box 123, Broadway, Sydney, NSW 2007, Australia
e-mail: uts.edu.au@gmail.com; Qiang.Yu@uts.edu.au

Keywords Forest fire · Fire danger indices · Fire risk probability · Semiparametric logistic regression

1 Introduction

Forest fires are a serious problem and have caused enormous social, environmental, and economic damage in China (Nbs 2011). Wildfires in contrasting climates in China are concentrated in different seasons and reflect weather-related effects.

The fire pattern is influenced by climate change (Thonicke and Cramer 2006). Weather is an important factor that influences forest fires (Moritz 2003; Taylor et al. 2008; Vasilakos et al. 2009). Fuel moisture content is controlled by species characteristics, climatic parameters, and environmental parameters (Castro et al. 2003; Viney 1991) and is considered a critical factor influencing fire ignition and distribution (Chandler et al. 1983). Therefore, several meteorological indices related to both meteorological parameters and soil water content variability have been developed to model the moisture dynamics of fuel (Keetch and Byram 1968; Turner and Lawson 1978). Different fire danger rating systems based on different meteorological variables have been developed in different locations, such as the National Fire Danger Rating System (NFDRS) (Deeming et al. 1977), Fire Weather Index (FWI) (Van Wagner 1977), and McArthur Forest Fire Danger Index (FDI) (McArthur 1967), quantified by Noble et al. (1980). In these systems, different fire weather indices are included for estimating fire risk, such as the Keetch–Byram Drought Index (KBDI) of the NFDRS (Deeming et al. 1977), Fine Fuel Moisture Code (FFMC), Duff Moisture Code (DMC), Drought Code (DC) of the FWI, drought factor (DF and DG), and Forest Fire Danger Index (FFDI) of the FDI (Griffiths 1999; Noble et al. 1980). In addition, the vegetation index such as normalized difference vegetation index (NDVI) derived from satellite images is a good indicator of greenness of vegetation, water stress, and other vegetation parameters (Zhou et al. 2003). Recently, NDVI has been typically used to assess fire danger (Cheret and Denux 2011; De Angelis et al. 2012; Wang et al. 2013).

Numerous studies report the relationships between fire danger indices and fire characteristics. Logistic regression was used to assess the predictability of fire danger indices on the probability of fire days (Anderson et al. 2000; Catry et al. 2009). Poisson model was used to evaluate the relationship of fire weather indices and fire frequency (Mandallaz and Ye 1997). Stepwise regression was used to assess the ability of fire weather indices to estimate the relationship between fire frequency and area burned (Carvalho et al. 2008). The relationship between fire occurrences and fire danger indices with temporal variables was studied from time-since-last-fire data (Grissino-Mayer 1999; Peng and Schoenberg 2001). Logistic regression with fire danger indices and spatial variables as explanatory variables was used to study spatial autocorrelation between proximal fires (Chou et al. 1993). Nonparametric or semiparametric logistic regression with spatially and temporally explanatory variables was used to evaluate the ability of fire danger indices to estimate the probability of fire ignition and large fire events (Brillinger et al. 2006; Preisler et al. 2008).

Several fire danger indices such as DF, DG, FFDI, FWI, and FFWI were introduced in some locations in China (Tian et al. 2009; Yang et al. 2010; Zhao et al. 2009), but no research has been conducted on the relationships between fire danger indices and forest fire activity in contrasting climates in China (Shu et al. 2003). In the present study, to assess the ability of fire danger indices to estimate the probability of fire occurrence in contrasting

climates, the semiparametric logistic regression (Brillinger et al. 2006; Preisler et al. 2008) was used in four contrasting climatic regions in China on a 1×1 degree \times day scale. A previous study published in 2012 focused on the same objective but on a monthly scale. In this study, the predictive ability of fire danger indices was analyzed on a daily scale. Partial effect plots were used to analyze the relationship between fire danger indices and fire ignition probabilities. With selected fire danger indices, as well as spatially and temporally variables as explained variables, probability models were established to estimate probability of fire ignition in each climatic region on daily scale.

2 Materials and methods

2.1 Study area

The four regions used in this study are North China (NR), Northeast China (NE), Southeast China (SE), and Southwest China (SW) (Fig. 1). Each region is influenced by different atmospheric circulation, climate, and monsoon patterns. Table 1 contains a list of properties on fire pattern, climate, and vegetation. The four regions have different fire patterns which are due to spatial variation in the occurrence of drought, wind speed, precipitation patterns, temperature, and accumulated snow. Given the gentle topography and influence of the monsoon in spring and autumn, the seasonality of high forest fire danger among the four regions is varied. Forest fires in NE spread quickly and over large areas, but at low frequency. By contrast, in the SE and SW, the forest fire frequency is high but the burnt area is small.

In NR, locust trees (*Robinia pseudoacacia* L.) and littleleaf peashrub (*Caragana microphylla* Lam.) are the most common species. In NE, rainfall is less than in southern parts of China. Summers are short, warm, and humid, whereas winters are long, cold, and dry with snow covering the forest floor for approximately 6 months between November and late April (Zhou et al. 1991). NE is an important forestry region in China, and it includes the southern extension vegetation of eastern Siberian boreal forests (Zhou et al. 1991). Birch (*Betula platyphylla* Sukaczew) and pine (*Pinus sylvestris* L. var. *mongolica* Litv.) mixed with larch (*Larix gmelini* Rupr.) are the major species that influence fire disturbance and forest harvesting in NE (Xu 1998). SE is within a transitional subtropical vegetation zone with a warm and wet humid weather in summer and a cooler drier weather in winter (Box 1995). Considering deforestation and land-use conversion to agricultural production, some remnant forests have almost disappeared and numerous pine and Eucalyptus plantations have appeared in the region. In SW, vegetation is mainly composed of mixed rain forest with high biodiversity and dipterocarp rain forest (Pu et al. 2001).

2.2 Meteorological data and NDVI data

Two-hundred forty-five weather stations covering the majority of the four different climate regions were selected in our study (Fig. 1). The daily precipitation, daily maximum temperature, daily average temperature, daily wind speed, and daily relative humidity of these weather stations between 1996 and 2008 were obtained from the Chinese Meteorological Administration for calculation of fire weather indices. For the present study, FWI components were computed using daily maximum temperature, daily relative humidity, and daily wind speed instead of noon values of these weather parameters.

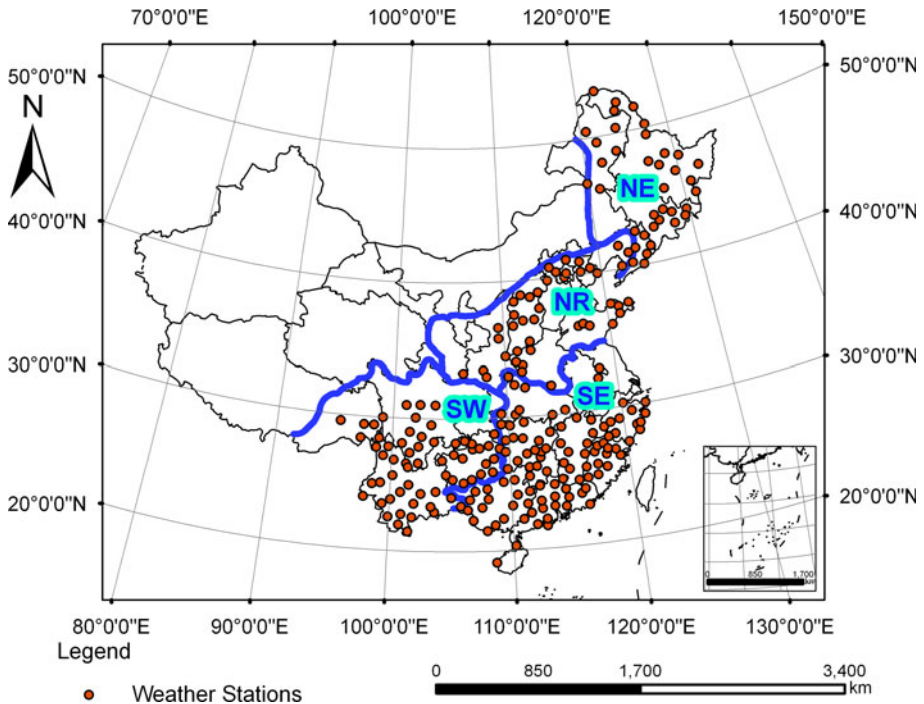


Fig. 1 Distribution of study areas and weather stations. NE, NR, SE, and SW represent Northeast China, North China, Southeast China, Southwest China, respectively

The NDVI values used in the study were extracted from spot vegetation NDVI data and GIMMS-NDVI-China data, which were obtained from the Environmental and Ecological Scientific Data Center of Western China, National Natural Science Foundation of China (<http://westdc.westgis.ac.cn>).

2.3 Fire occurrence data

The fire occurrence data used in our study were downloaded from the European Space Agency (ESA). The database also includes fire information concerning spatial coordinates, ignition date, land cover classification, and biomass burned. These data were obtained from the Along Track Scanning Radiometer (ATSR) World Fire Atlas (ESA, ATSR World Fire Atlas, available at <http://dup.esrin.esa.int/ionia/wfa/index.asp>) and Data User Element of the ESA. The ATSR instrument has a spatial resolution of 1 km × 1 km. All hot spots (including gas flares) with high temperature at night are precisely located using the 3.7- μm thermal channel. Fire detection algorithm 2 (hot spot if: 3.7 μm > 308 K) was used for the ATSR data. The detailed description of the fire detection algorithm is available at the ESA Web site (<http://dup.esrin.esa.int/ionia/wfa/index.asp>). However, problems with these data include ATSR frame overlap (some fires can be detected twice) and global underestimation of the hot spot frequency (only night time fires are detected). Consequently, we removed the obvious duplicated records and assume that the visualizations of the data reflect real patterns but with possible underestimates because of occasional day-only fires. The fire database used comprised data from 1996 to 2008.

Table 1 Climate and vegetation conditions in the four regions

	NR	NE	SE	SW
Regional climate	Temperate climate	Cold temperate and frigid climate	Humid subtropical and tropical climate	Tropical and subtropical climate
Dominant monsoon or air mass	Pacific Ocean monsoon	Siberian cold air mass	Pacific Ocean monsoon	Indian Ocean monsoon, Pacific Ocean monsoon
Annual mean T (°C)	7–16	-5–5	16–20	12–16
Summer T (°C)	26	17	35	20
Winter T (°C)	-7	-29	-3	7
Annual rainfall (mm)	400–900	400–650	1,300–1,900	1,100
Seasons with 70 % of seasonal rainfall	April–November	June–August	April–September	May–October
Seasons with 30 % of seasonal rainfall	December–March	November–March	December–February	November–March
Fire seasons	May–July	March–July, October	October–April	January–May
Vegetation	Deciduous broad-leaved forest	Cool temperate coniferous forests	Evergreen broadleaf forest, Deciduous broad-leaved forest	Tropical rain forest

2.4 Fire danger indices

We used observed data from the weather stations to calculate daily fire weather indices. Table 2 lists the fire weather indices and their input weather variables used in our study (Fosberg 1978; Griffiths 1999; Keetch and Byram 1968; Noble et al. 1980; Van Wagner 1970, 1987; Williams 1959). To analyze the influence of vegetative seasonal changes on fire ignition, we added NDVI as an explanatory variable in the probability model. NDVI is a normalized difference between near infrared and red channels. NDVI can be extracted from satellite sensor data using a combination of visible and near-infrared light reflected by vegetation.

2.5 Statistical analysis

We used the probability of fire ignition as a measure of fire danger. The probability of fire ignition was the probability of at least one fire occurring on a given day in a specific 1×1 degree grid cell with the weather station as the center. A semiparametric logistic regression model (Brillinger et al. 2006; Hastie et al. 2001) was used to estimate the fire ignition probability for each study region:

$$\text{logit}(p_t) = \beta_0 + \alpha_t + g_1(\text{lon}_t, \text{lat}_t) + g_2(\text{day}_t) + g_3(\text{altitude}_t) + \sum_{n=1} h_n(X_{nt}) \quad (1)$$

where the subscript t indicates the 1×1 degree \times day voxel with each weather station as the center. Each 1×1 degree grid cell was formed around each existing weather station. Two-hundred forty-five weather stations covering the majority of the four different climate regions were selected in our study. Given the 1×1 degree grid cell formed around each existing weather station, we only used the fire data for the same 1×1 degree grid cell. p is the probability of fire ignition; $\alpha_t = \log(I/s)$; s is the sampling proportion for nonfire locations; (lon, lat) are the latitude and longitude of the weather station of the 1×1 degree \times day grid cell; day is the day in a year; altitude is the altitude (in meters) at a specific location; and X_n are explanatory variables (e.g., the aforementioned fire danger indices). The functions $g_i()$ and $h_n()$ are nonparametric smoothing functions (e.g., piecewise polynomials and splines) that characterize the nonlinear relationships between the explanatory variables and logit of fire probability better than parametric functions. Considering that the data set was very large, a sample of nonfire locations was used. All voxels with fires and a proportional sample of voxels with no fires for each day were used for analysis.

Akaike information criterion (AIC) (Sakamoto et al. 1986) statistics were used to choose between indices based on their ability to estimate the probability of fire. We used AIC statistics to compare the historic model (H) and fire danger index model (named after the index). For H, location and day were the only explanatory variables. For the fire danger index model, location, day, and one fire danger index were the explanatory variables. According to the AIC statistics for each index, we developed the final regression model based on H by adding the “best” selection of indices with low AIC and only if the indices achieved a significance level of 0.05. The final regression model was used to estimate fire ignition probability via cross-validation for each region. The partial effect plots produced by the GAM module were analyzed to estimate the spline functions used in the final models. All estimations were done with the R statistical package (R Development Core Team 2013).

Table 2 Fire weather indices used in the study

Fire indices	Weather data	Country popularly used	Description
The Fine Fuel Moisture Code (FFMC) (Van Wagner 1977)	R, T, RH	Canada	Moisture content of fine fuels
The Duff Moisture Code (DMC) (Van Wagner 1977)	R, T, RH, L_e	Canada	Moisture content of loosely compacted organic material
The Drought Code (DC) (Van Wagner 1977)	R, T, L_f	Canada	Moisture content of a deep layer of compact organic material
The Initial Spread Index (ISI) (Van Wagner 1977)	R, T, RH, V	Canada	A combination of wind and FFMC that estimates the potential spread rate of a fire
The Build-up Index (BUI) (Van Wagner 1977)	R, T, RH, L_e, L_f	Canada	A combination of the DMC and DC that represents the availability of fuel for consumption
The Fire Weather Index (FWI) (Van Wagner 1977)	R, T, RH, L_e, L_f, V	Canada	A combination of the ISI and BUI that estimates the potential intensity of a spreading fire
The Daily Severity Ratio (DSR) (Van Wagner 1977)	R, T, RH, L_e, L_f, V	Canada	A power function of the FWI to increase the weight of higher values of FWI was added in FWI
The Fosberg Fire Weather Index (FFWI) (Fosberg 1978)	V, T, RH	America	The Fosberg Fire Weather Index
The Keetch-Byram Drought Index (KBDI) (Keetch and Byram 1968)	T_{max}, R	America	The Keetch-Byram Drought Index describing the soil moisture deficit
The McArthur Forest Fire Danger Index (FFDI) (McArthur 1967)	T_{max}, RH_{min}, V	Australia	The McArthur forest fire danger meter
The Drought Factor of the FDI (DG) (Griffiths 1999)	T_{max}, R	Australia	The Griffiths (1999) equation for the drought factor

T and RH refer to air temperature and relative humidity. The subscripts min and max denote daily minimum and maximum values of these quantities. V and R are wind speed and daily precipitation. L_e and L_f are effective day length in DMC and day length adjustment in DC , respectively

We used graphs of observed versus estimated probabilities to assess the accuracy of fit of the final selected models (Hosmer and Lemeshow 1989). According to similar linear predictors, all grid cells were grouped, and the observed fraction of fire ignitions in each group was compared with the average estimated probability for that group.

Two practical outputs of the final regression models are presented in this study. One is the fire danger maps (Preisler et al. 2004) based on estimated probabilities of fire ignition in a given 1×1 degree \times day voxel. The probabilities of fire ignition in the sampled 245 1×1 degree \times day grid cells were originally estimated by regression model, and then, a weighted inverse distance method was used to interpolate the probabilities to the 1×1 degree \times day voxel level in areas with no weather station. In our study, we present fire danger maps for May 01, 1997, and April 30, 2005, as examples and compare the estimated fire danger probabilities with observed fire events in these maps.

Another practical output is the expected fire ignition frequency for a given region and time period. In our study, the expected fire ignition frequency was calculated by summing the estimated probabilities over individual voxels of each study region and days of each month. The monthly estimated probabilities and approximate confidence intervals were also calculated for that given region and period.

3 Results

The AIC statistics for H and fire danger index models were plotted for each region. All AIC values are relative to the AIC values of H model (set to zero in each region). The effects of fire danger indices on fire ignition probabilities in contrasting climates were compared through the AIC statistics. Figure 2 shows the relative importance of each index on the fire ignition probabilities in each region on a daily scale. Different regions had different indices which were most strongly associated with fire ignition. Altitude, ISI, FFMC, and FWI in NR; FWI, FFMC, ISI, and DSR in NE; FFMC, FWI, ISI, and FFDI in SE; FFMC, ISI, FWI, and FFDI in SW were the indices most strongly associated with fire ignition.

For each region, the final regression model was developed by adding the H model and selected indices with low AIC and only if they achieved the significance level of 0.05. Variables selected in the final regression model were different in each region except for location and day. Figure 3 shows the estimated partial effects of spatial location in each region. The partial effects are the estimates of the nonparametric functions describing the effect of each variable on fire danger probability in the model. Spatial location had highly significant effects in all four regions. The estimates suggest that probabilities of fire ignition are highest in the middle portion of NR, in the northern part of NE, in the southeastern part of SE, and in the southern part of SW.

In NR, the probability of fire ignition increased linearly as FWI increased (Fig. 4c). The probability of fire ignition increased with increase in FFMC, $\text{KBDI} < 150$, and $\text{NDVI}_{\text{gimms}} < -0.6$, but decreased with increase in $\text{NDVI}_{\text{gimms}} > -0.6$. The relationship between fire ignition probability and altitude is nonlinear (Fig. 4b). Fires more often occur when altitude values are $> 2,000$ m and less often occur when altitude values are between 1,500 and 2,000 m. Figure 4a indicates more fires in the summer in NR.

In NE, probability of fire ignition increased linearly as FWI increased (Fig. 5d). Estimated probability of fire ignition increased with increase in $\text{ISI} > 15$, $\text{FFDI} < 24$ and $\text{DSR} > 40$, and $\text{NDVI}_{\text{spot}}$, but decreased with increase in $\text{FFDI} > 24$. Figure 5a indicates that probabilities of fire ignition are high in spring and autumn in NE.

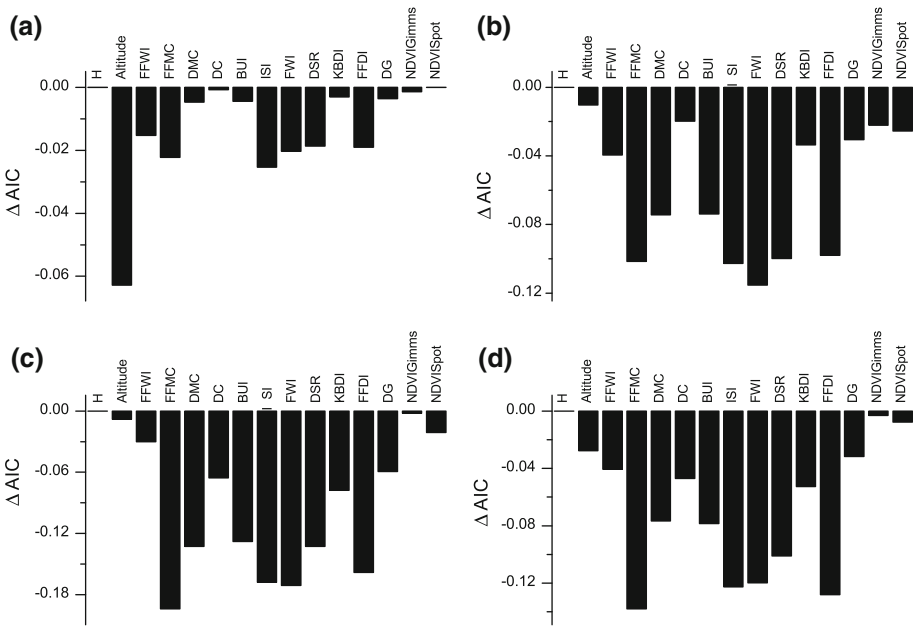


Fig. 2 AIC statistics describing the relative importance of each fire danger index on the probabilities of fire occurrence for H model and fire danger index models in **a** NR, **b** NE, **c** SE, and **d** SW. All AIC values in the plots are relative to AIC values of H models which were set to zero in each region, i.e. $(AIC_{index} - AIC_H) / AIC_H$

In SE, probability of fire ignition increased linearly with increased ISI and FFMC (Fig. 6). Estimated probability of fire ignition increased with increase in DC < 700 and NVDIspot -0.3 , but decreased with increase in DC > 700 and NVDIspot <-0.3 . The relationship between fire ignition probability and altitude is nonlinear (Fig. 6b). Fires more often occur when altitude is between 400 m and 900 m, and >1,500 m, but less often occur when altitude is between 900 m and 1,500 m. Figure 6a indicates that probabilities of fire ignition are high in winter and spring in SE.

In SW, fires more often occur when altitude is between 500 m and 1,800 m and less often occur when altitude >1,800 m (Fig. 7b). Probability of fire ignition increased linearly with increased FWI and FFMC (Fig. 7d, e). Estimated probability of fire ignition increased with increased FFDI and KBDI (Fig. 7c, f). Figure 7a indicates that probabilities of fire ignition are high in spring in SW.

Seven explanatory variables (i.e., spatial location, day in a year, altitude, FWI, FFMC, KBDI, and NDVIgimms) had highly significant effects on fire ignition in NR (Fig. 4). In NE, spatial location, day in a year, ISI, FFDI, FWI, DSR, and NDVIspot had highly significant effect on fire ignition probability (Fig. 5). Figure 6 shows the estimated partial effects of significant variables in SE. Seven explanatory variables (i.e., spatial location, day in a year, altitude, ISI, FFMC, DC, and NDVIspot) had highly significant effect in SE (Fig. 6). In SW, spatial location, day in a year, altitude, FFDI, FWI, FFMC, and KBDI had highly significant effects on fire ignition (Fig. 7).

The plots in Figs. 4, 5, 6, and 7 could be used to predict days with higher than average probabilities of fire ignition in the four regions. As indicated in Fig. 4, when FWI values are >15, FFMC values >70, KBDI values >90, and NDVIgimms values <0.1, the model

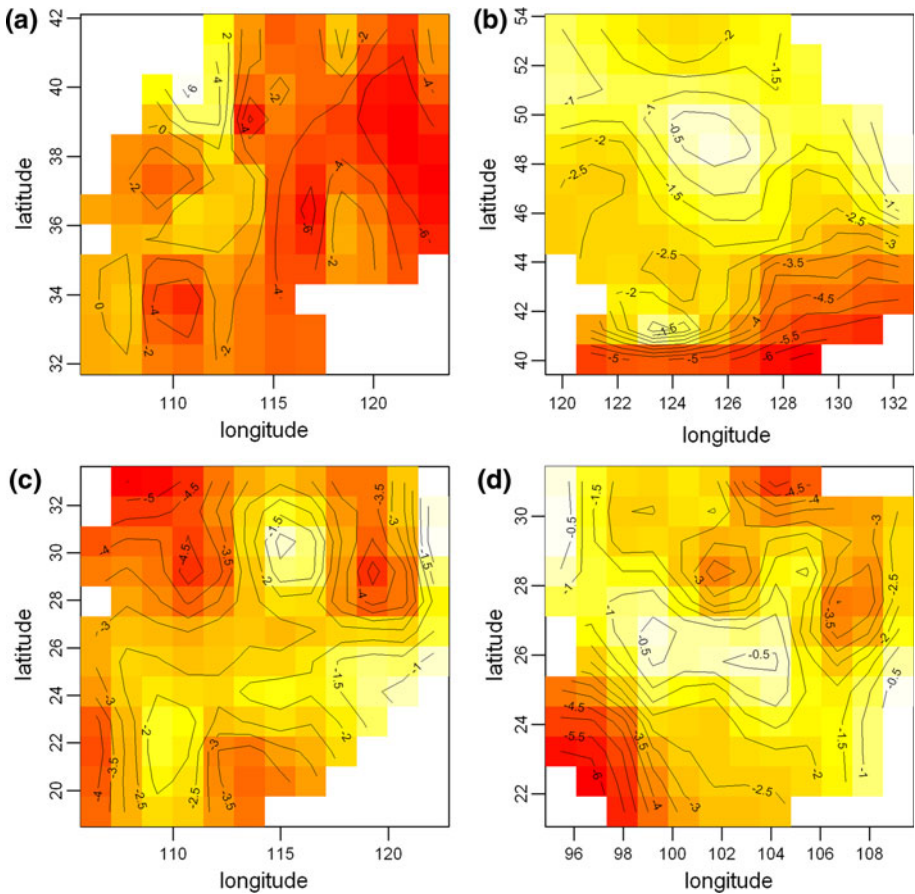


Fig. 3 Estimated partial effects of location on the probability of fire ignition in **a** NR, **b** NE, **c** SE, and **d** SW

predicts higher than average probabilities of fire ignition in NR. According to the plots in Fig. 5, when $ISI > 30$, $FFDI > 5$, $FWI > 15$, $DSR > 50$, and $NDVI_{spot} > 0.2$, the model predicts higher than the average probability of fire ignition in NE. Figure 6 shows that when $ISI > 5$, $FFMC > 70$, $DC > 300$, and $NDVI_{spot} > 0.2$, the model predicts higher than the average probability of fire ignition in SE. In SW, when $FFDI > 6$, $FWI > 15$, $FFMC > 70$, and $KBDI > 150$, the model predicts higher than the average probability of fire ignition (Fig. 7).

To assess the ability of the final regression models to estimate the probability of fire ignition in the four regions, we plotted the graphs of observed relative frequencies of fires versus estimated probabilities grouped by similar linear predictor in Fig. 8. The larger confidence bounds for larger linear predictors may be attributed to the small number of cases. Most of the observed points fall inside the estimated point-wise 95 % confidence bounds from the final model in NE, SE, and SW. However, some points fall outside the estimated point-wise 95 % confidence bounds from the final model in NR, which is partially because high fire danger is not always associated with fire occurrence, and external factors such as human behavior (land-use policy, fire suppression strategy,

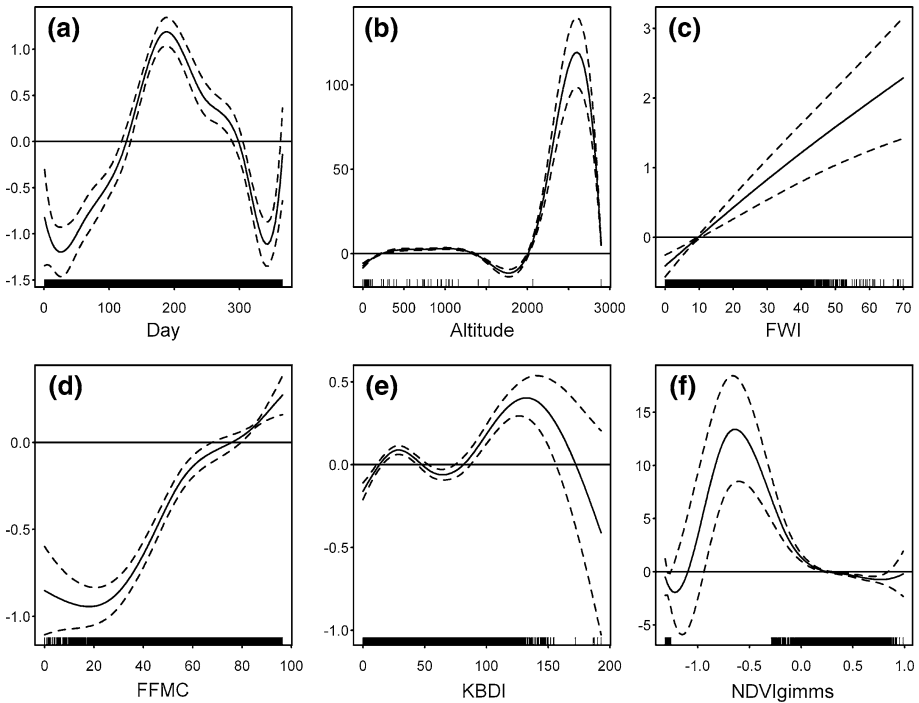


Fig. 4 Estimated partial effects of significant variables on the probability of fire ignition in NR

etc.) are not considered in the model computation. The range of estimated probabilities according to the final model is 0–0.53 in NR, 0–0.99 in NE, 0–0.99 in SE, and 0–0.85 in SW. For a probability model, more accurate estimating ability is associated with larger estimated probability range. Although few observed points fall outside confidence bounds, the fit of the final models in the four regions is reasonable. The observed points that fall outside confidence bounds may disappear with other variables included in the models.

To show several outputs from the final models in the four regions, we plotted fire danger maps with estimated probabilities and observed fire events for May 01, 1997, and April 30, 2005 (Fig. 9). The fire danger maps indicate that the fire ignition probabilities were higher on May 01, 1997, than on April 30, 2005, in NE but were similar in NR, SE, and SW. The probabilities of fire ignition were relatively higher in NE, middle portion of NR, and middle portion of SW on May 01, 1997. In addition, the probabilities of fire ignition were relatively higher in the southern part of NE, northern part of NR, western part of SE, and southern part of SW on April 30, 2005. On both maps, the points of observed fire ignition events were mostly located in grid cells with relatively higher fire risk probabilities. The maps show good predictive results in NE and SW. For estimated probabilities of fire ignition which indicated fire risk but no real fire ignition occurred, the grid cells with relatively higher fire risk probabilities may be consistent with nonobserved fire ignition, as shown in NR and SE.

A practical output of the probability model is the average monthly estimated fire frequency calculated from daily estimations. This frequency was plotted in each region (Fig. 10) and calculated by adding all the probabilities in every voxel in each day in the

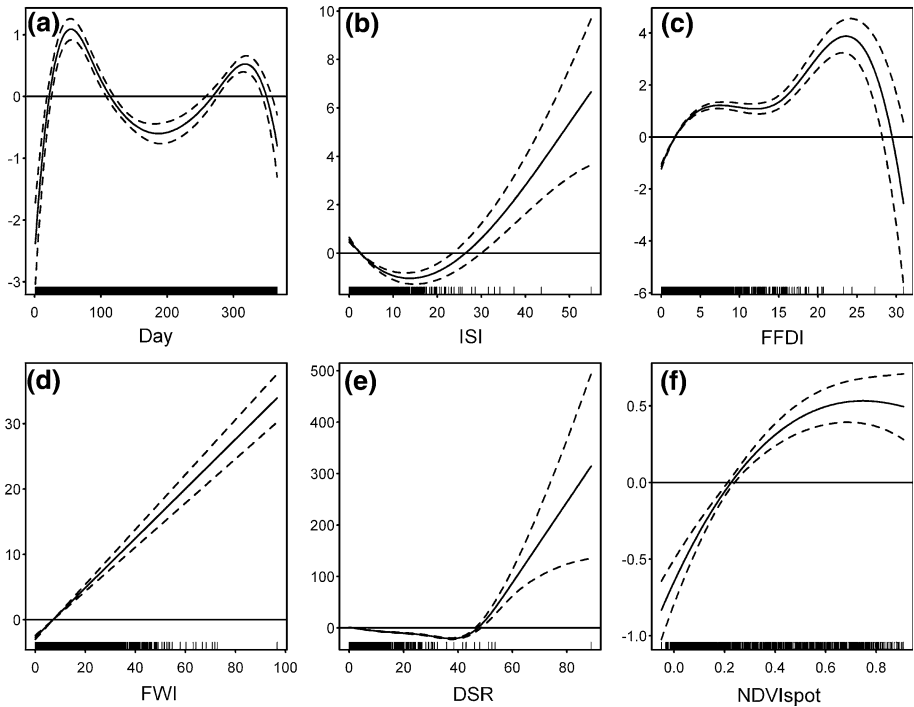


Fig. 5 Estimated partial effects of significant variables on the probability of fire ignition in NE

region for each month and averaging the calculated results for the same months. In Fig. 10, estimated 95 % confidence limits, observed fire ignition frequency, and 2 SE limits for the dots are also plotted. The approximate 95 % bounds are obtained by the jackknife procedure (Efron and Tibshirani 1993). The dots in Fig. 10 refer to the naive estimate of the rates of fires obtained by dividing the total fire frequency for a month by the number of years of observation. The vertical lines show 2 SE limits employing a Poisson approximation. The estimated fire ignition frequency peaks in different seasons in the four regions. The estimated fire frequencies peak in June (40.5) in NR, May (20.3) in NE, December (33.9) in SE, and March (43.1) in SW. The final models produced good results in NE and SE. The two points of observed fire frequencies which fall outside the estimated 95 % confidence bounds in NR and SE, respectively, may be attributed to other variables affecting fire ignition.

4 Discussion

Results show that the semiparametric logistic regression model is useful for estimating fire risk and for assessing the ability of fire danger indices to estimate probabilities of fire ignition on a daily scale. The four regions had different significant indices which explained the variance of fire ignition probabilities. The difference was partly because of the different local weather and vegetation conditions.

Location and day in a year were highly significant variables in the final models in the four regions. At least until other additional indices diminish the significance of these

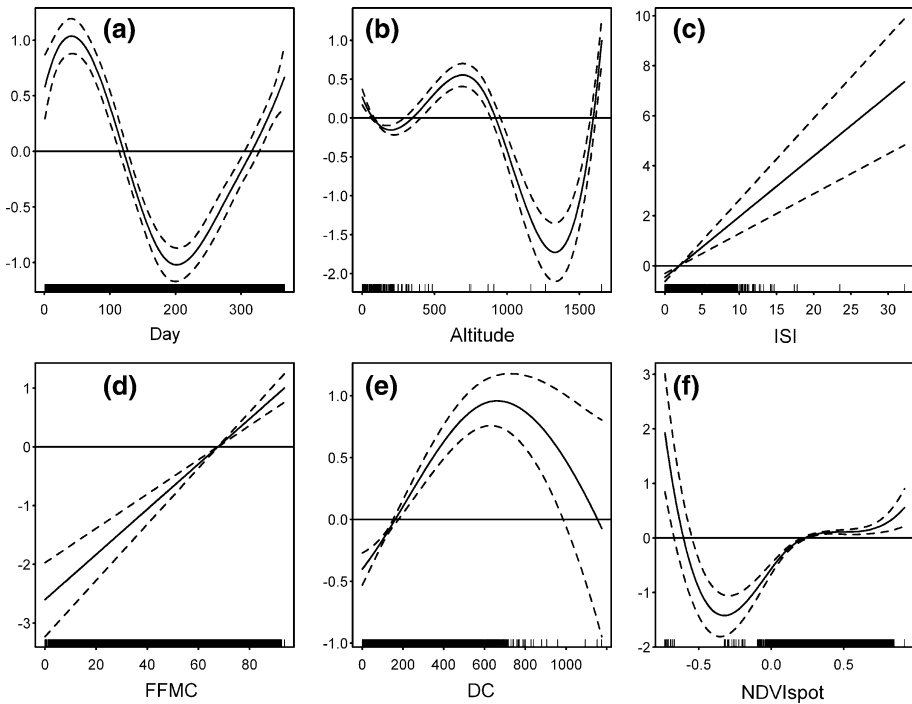


Fig. 6 Estimated partial effects of significant variables on the probability of fire ignition in SE

variables, they are necessary in the probability model as proxies for variables with spatial patterns consistent over time and with annual cyclical patterns that are not properly represented by fire danger indices.

The selection of fire danger indices as explained variables in the final probability models indicated the influence of danger indices on fire ignition. On a daily scale, altitude showed an influence on fire ignition, and thus on fire occurrence, in NR, SE, and SW. Altitude was not the significant index in the final probability model in NE on a daily scale. NDVI was selected as explained variable in NR, NE, and SE on fire ignitions. The selection of NDVI in the three regions indicated that the interannual influence of vegetation variations on fire ignition should be reflected by other vegetation indices in these regions. According to the low significance of NDVI in the model of this region, the interannual changes of vegetation did not influence fire ignition on a daily scale in SE. According to the selection of FFM as explained variable in the final model, fine fuel moisture is an important factor that influences fire occurrence in NR, SE, and SW. The selections of FFM and DC in SE indicated that fuel moisture of two fuel layers is involved in fire ignition in the region. According to the selection of ISI in the final models, wind speed showed an influence on fire ignition on a daily scale in NE and SE. For the selection of KBDI in NR and SW models, extreme temperature is important in fire ignition on a daily scale. Thus, fire ignition in NR and SW is probably more critical in future scenarios involving global warming. Moreover, the present study serves as baseline information for future studies to predict the fire risk probability in these areas under future global warming scenario.

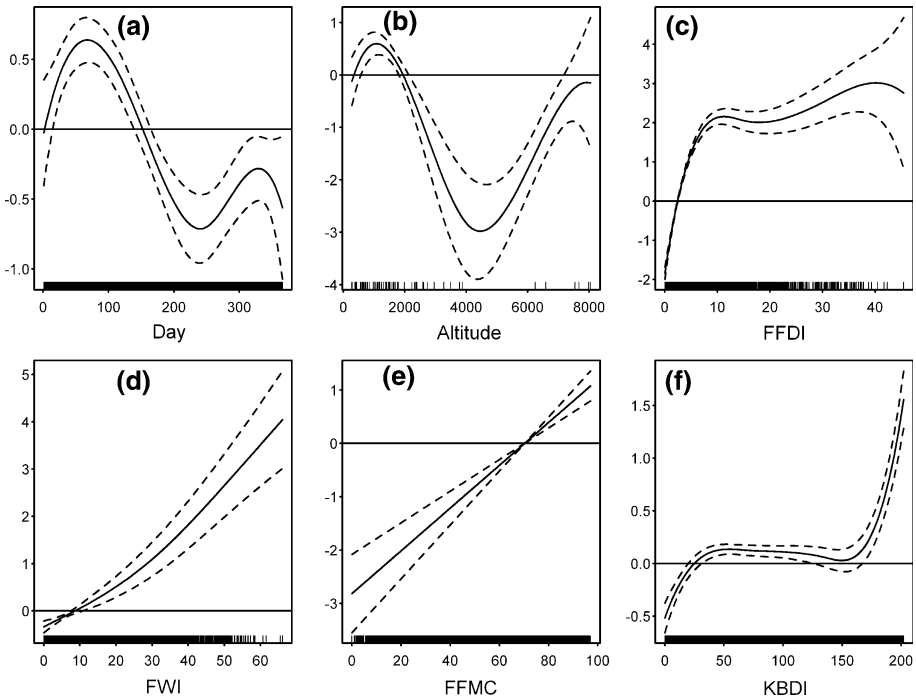


Fig. 7 Estimated partial effects of significant variables on the probability of fire ignition in SW

The predictive ability of the final models was different among the four regions which is partially consistent with the different use of fire danger indices in each region. When the estimated and observed probabilities of fire ignition in similar linear predictor levels were compared, the results of the probability models used in NE, SE, and SW were better than in NR on a daily scale. The estimated fire frequency calculated from the final models in NR and SW overestimated the fire events in the months of May and June, respectively. This overestimation may be partially attributed to factors other than weather and vegetation indices used in the probability models. The fire danger maps produced in our study were useful for personnel to predict the probabilities of fire ignition and minimize missed fire events.

In the study of fire danger risk, point-to-point temporal correlation statistics was a poor method to describe the nonlinear relationship between fire danger indices and fire frequency. Furthermore, correlation statistics are not adequate to analyze variables with small counts such as forest fire (mostly 0 or 1). By contrast, the partial effect plots of the significant variables used in our study were an effective method to analyze the nonlinear relationship between fire danger indices and fire ignition probability.

The semiparametric logistic regression model used in our study is a possible alternative method to predict fire ignition probability. This result is consistent with previous findings in other regions (Brillinger et al. 2006; Preisler et al. 2008).

In future studies, other temporal and spatial variables will be added in the probability models to improve the predictive ability. More accurate and updated fire information may also improve the probability model when used at a local level.

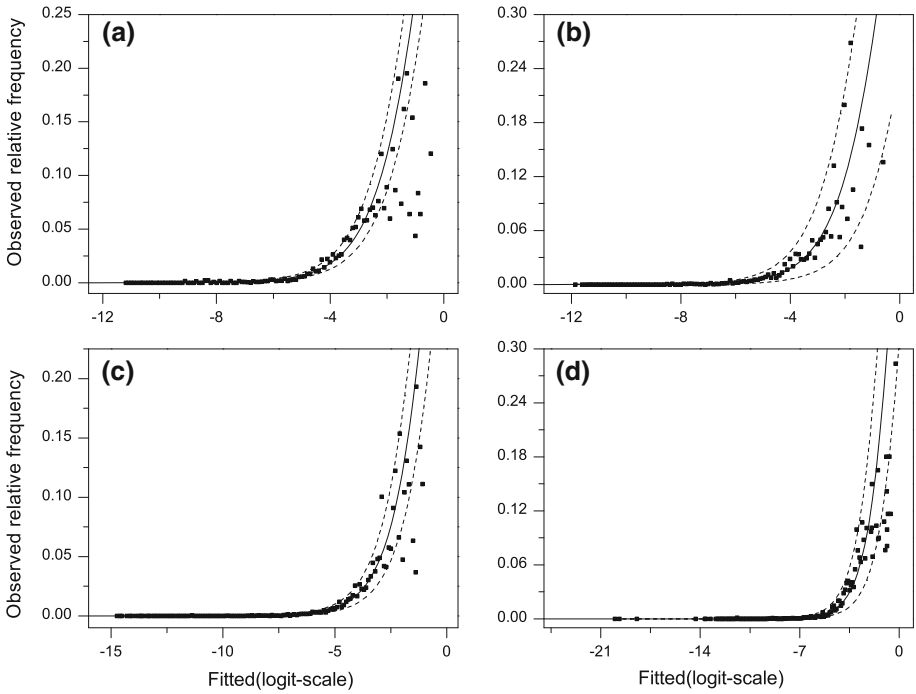


Fig. 8 Observed relative fire frequency grouped according to similar linear predictors in **a** NR, **b** NE, **c** SE, and **d** SW. *Solid lines* represent the estimated probabilities from the final models and *broken lines* represent the approximate binomial 95 % confidence bounds

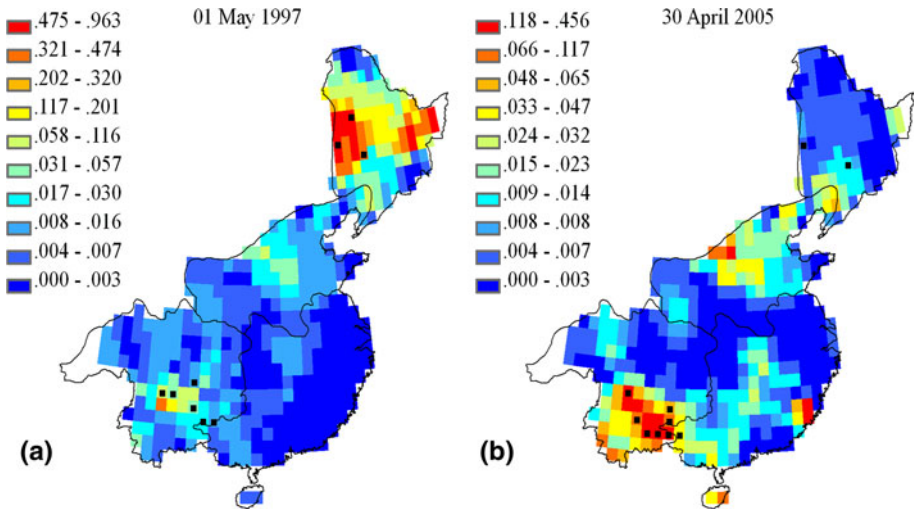


Fig. 9 Estimated probabilities of fire ignition compared with observed fire events (*dots*) for **a** May 01, 1997 and **b** April 30, 2005

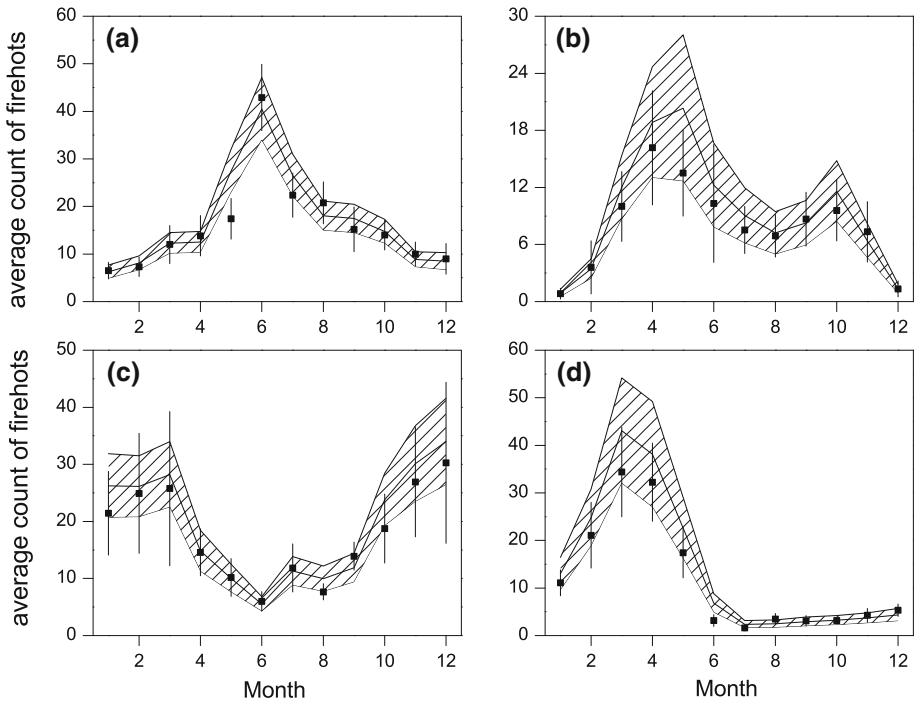


Fig. 10 Average monthly estimated fire ignition frequency in **a** NR, **b** NE, **c** SE, and **d** SW. Shaded regions show estimated 95 % confidence limits. The points are the observed fire ignition frequency and vertical lines are the 2 SE limits for the points

5 Conclusions

In this study, we demonstrated the feasibility of modeling and mapping fire ignition probability in contrasting climates using fire danger indices on a daily scale. We considered probability models and fire danger maps as effective methods to predict the probability of fire ignition in China. Results indicate the following statements. (1) Different fire danger indices were selected as significant variables dependent on the region. The inter-regional difference could be partially explained by difference in local weather and vegetation conditions. (2) Spatial location had highly significant effects in all four regions. NDVI values were selected as explained variable for NR, NE, and SE on fire ignitions. On a daily scale, altitude showed an influence on fire ignition for NR, SE, and SW. (3) The robustness of the probability models used in NE, SE, and SW was better than in NR on a daily scale. The semiparametric logistic regression model used in this study is useful for assessing the ability of fire danger indices to estimate probabilities of fire ignition on a daily scale. This study encourages further research on assessing the predictive ability of fire danger indices developed at other temporal and spatial scales in China.

Acknowledgments This work was supported by National Basic Research Program of China (No. 2010CB428404). The authors would like to thank their colleagues at the Institute of Geographic Sciences and Natural Resources Research, CAS, and University of Technology Sydney for their cooperation; and three anonymous referees are acknowledged for their review comments and suggestions in an earlier version of the manuscript.

References

- Anderson K, Martell DL, Flannigan MD, Wang D (2000) Modeling of fire occurrence in the boreal forest region of Canada. In: Kasischke E, Stocks BJ (eds) *Fire, climate change, and carbon cycling in the boreal forest*. Springer, New York, pp 357–367
- Box EO (1995) Climate relations of the forests of east and Southeast Asia. In: Box EO, Peet RK, Masuzawa T, Yamada I, Fujiwara K, Maycock PF (eds) *Vegetation science in forestry*. Kluwer, Dordrecht
- Brillinger DR, Preisler HK, Benoit JW (2006) Probabilistic risk assessment for wildfires. *Environmetrics* 17:623–633. doi:10.1002/ENV.768
- Carvalho A, Flannigan MD, Logan K, Miranda AI, Borrego C (2008) Fire activity in Portugal and its relationship to weather and the Canadian Fire Weather Index System. *Int J Wildland Fire* 17(3):328–338. doi:10.1071/wf07014
- Castro FX, Tudela A, Sebastia MT (2003) Modeling moisture content in shrubs to predict fire risk in Catalonia (Spain). *Agric For Meteorol* 116(1–2):49–59. doi:10.1016/S0168-1923(02)00248-4
- Catry FX, Rego FC, Bacao F, Moreira F (2009) Modeling and mapping wildfire ignition risk in Portugal. *Int J Wildland Fire* 18:921–931
- Chandler P, Cheney P, Thomas L, Trabaud L, Williams D (1983) *Fire in forestry*, vol 1. Wiley, New York
- Cheret V, Denux JP (2011) Analysis of MODIS NDVI time series to calculate indicators of mediterranean forest fire susceptibility. *GISci Remote Sens* 48(2):171–194. doi:10.2747/1548-1603.48.2.171
- Chou YH, Minnich RA, Chase RA (1993) Mapping probability of fire occurrence in San Jacinto Mountains, California, USA. *Environ Manag* 17(1):129–140
- De Angelis A, Bajocco S, Ricotta C (2012) Modelling the phenological niche of large fires with remotely sensed NDVI profiles. *Ecol Model* 228:106–111. doi:10.1016/j.ecolmodel.2012.01.003
- Deeming JE, Burgan RE, Cohen JB (1977) *The national fire-danger rating system-1978*. USDA, Forest Service, Gen. Tech. Rep., vol 39. Intermountain Forest and Range Experiment Station, Ogden, UT, USA
- Efron B, Tibshirani RJ (1993) *An Introduction to the Bootstrap*. Chapman Hall, New York
- Fosberg MA (1978) Weather in wildland fire management: the fire weather index. Paper presented at the Conference on Sierra Nevada Meteorology, Lake Tahoe, CA, June 19–21
- Griffiths D (1999) Improved formula for the drought factor in McArthur's forest fire danger meter. *Aust For J* 62(2):210–214
- Grissino-Mayer HD (1999) Modeling fire interval data from the American Southwest with the Weibull distribution. *Int J Wildland Fire* 9(1):37–50
- Hastie TJ, Tibshirani R, Friedman J (2001) *The elements of statistical learning: data mining, inference, and prediction*. Springer, New York
- Hosmer DW, Lemeshow S (1989) *Applied logistic regression*. Wiley, New York
- Keetch JJ, Byram GM (1968) A drought index for forest fire control. USDA Forest Service Research Paper, vol 38. Forest Service Southeastern Forest Experiment Station, Asheville, North Carolina
- Mandallaz D, Ye R (1997) Prediction of forest fires with Poisson models. *Can J For Res* 27:1685–1694
- McArthur AG (1967) Fire behaviour in eucalypt forest. *Comm Aust For Timb Bur Leaflet* 107:25p
- Moritz MA (2003) Spatiotemporal analysis of controls on shrubland fire regimes: age dependency and fire hazard. *Ecology* 84:351–361
- Nbs (2011) The 2011 yearly data of National Statistics Database on the website of National Bureau of Statistics of China. Available online at <http://www.stats.gov.cn/tjsj/ndsj/2011/indexeh.htm>
- Noble IR, Bary GAV, Gill AM (1980) McArthur's fire-danger meters expressed as equations. *Aust J Ecol* 5:201–203
- Peng R, Schoenberg F (2001) Estimation of wildfire hazard using spatial-temporal fire history data. Statistics Department, University of California, Los Angeles
- Preisler HK, Brillinger DR, Burgan RE, Benoit JW (2004) Probability based models for estimating wildfire risk. *Int J Wildland Fire* 13:133–142. doi:10.1071/WF02061
- Preisler HK, Chen SC, Fujioka F, Benoit JW, Westerling AL (2008) Wildland fire probabilities estimated from weather model-deduced monthly mean fire danger indices. *Int J Wildland Fire* 17(3):305–316. doi:10.1071/wf06162
- Pu YS, Zhang JH, Cao M (2001) A strategic study on biodiversity conservation in Xishuangban. *J For Res* 12:25–30
- Sakamoto Y, Ishiguro M, Kitagawa G (1986) *Akaike information criterion statistics*. D. Reidel Publishing Company, Dordrecht
- Shu L, Zhang X, Dai X, Tian X, Wang M (2003) Forest fire research (II)-fire forecast. *World For Res* 16(4)
- Taylor AH, Trouet V, Skinner CN (2008) Climatic influences on fire regimes in montane forests of the southern Cascades, California, USA. *Int J Wildland Fire* 17(1):60–71. doi:10.1071/Wf07033

- R Development Core Team (2013) R: a language and environment for statistical computing. R Foundation for Statistical Computing, Vienna. Accessed available at <http://www.R-project.org>
- Thonicke K, Cramer W (2006) Long-term trends in vegetation dynamics and forest fires in Brandenburg (Germany) under a changing climate. *Nat Hazards* 38(1–2):283–300. doi:[10.1007/s11069-005-8639-8](https://doi.org/10.1007/s11069-005-8639-8)
- Tian XR, Shu LF, Wang MY, Zhao FJ (2009) Spatial and temporal distribution of lightning fire and forecasting model for Daxing'anling region. *Forest Res* 22(1):14–20
- Turner JA, Lawson BD (1978) Weather in the Canadian forest fire danger rating system. A user guide to national standards and practices, vol BC. BC-X-177. Environment Canada. Pacific Forest Research Centre, Victoria
- Van Wagner CE (1970) Conversion of William's severity rating for use with the Fire Weather Index. *Inf Rep Can For Serv*
- Van Wagner CE (1977) Conditions for the start and spread of crown fire. *Can J For Res* 7(1):23–34
- Van Wagner CE (1987) Development and structure of the Canadian forest fire weather index system. *Canadian For. Ser. Tech. Rep*
- Vasilakos C, Kalabokidis K, Hatzopoulos J, Matsinos I (2009) Identifying wildland fire ignition factors through sensitivity analysis of a neural network. *Nat Hazards* 50(1):125–143. doi:[10.1007/s11069-008-9326-3](https://doi.org/10.1007/s11069-008-9326-3)
- Viney NR (1991) A review of fine fuel moisture modelling. *Int J Wildland Fire* 1(4):215–234. doi:[10.1071/WF9910215](https://doi.org/10.1071/WF9910215)
- Wang L, Zhou Y, Zhou W, Wang S (2013) Fire danger assessment with remote sensing: a case study in Northern China. *Nat Hazards* 65(1):819–834. doi:[10.1007/s11069-012-0391-2](https://doi.org/10.1007/s11069-012-0391-2)
- Williams DE (1959) Fire season severity rating. Vol Forest Res. Div. Tech. Note. Can. Dep. Northern Aff. Nat. Resources
- Xu HC (ed) (1998) Da Hinggan Ling Mountain forests in China. Science Press, Beijing
- Yang G, Di XY, Zeng T, Shu Z, Wang C, Yu HZ (2010) Prediction of area burned under climatic change scenarios: a case study in the Great Xing'an Mountains boreal forest. *J For Res* 21(2). doi:[10.1007/s11676-010-0035-x](https://doi.org/10.1007/s11676-010-0035-x)
- Zhao FJ, Shu LF, Tiao XR, Wang MY (2009) Change trends of forest fire danger in Yunnan Province in 1957–2007. *Chin J Ecol* 28(11):2333–2338
- Zhou YL, Ai CL, Dong SL, Nie SQ, Yang GT, Zhou RC, Zhou WQ (eds) (1991) Vegetation of Greater Xingan in China. Scientific Press, Beijing
- Zhou W, Zhou Y, Wang S, Zhao Q (2003) Early warning for grassland fire danger in North China using remote sensing. Paper presented at the International geoscience and remote sensing symposium (IGARSS03), Toulouse, France, 21–25 July